

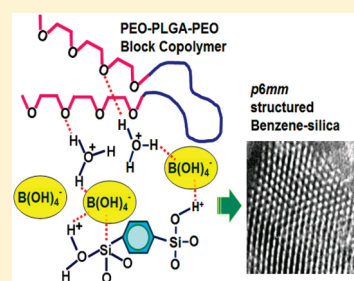
## Periodic Mesoporous Benzene–Silicas Prepared Using Boric Acid as Catalyst

Eun-Bum Cho,<sup>†,§</sup> Manik Mandal,<sup>‡</sup> and Mietek Jaroniec<sup>\*,§</sup><sup>†</sup>Department of Fine Chemistry, Seoul National University of Science and Technology, Seoul 139-743, Korea<sup>‡</sup>Department of Chemistry, College of Staten Island, City University of New York, New York 10314, United States<sup>§</sup>Department of Chemistry, Kent State University, Kent, Ohio 44242, United States

S Supporting Information

**ABSTRACT:** Highly ordered periodic mesoporous benzene–silicas with 2D  $p6mm$  symmetry were synthesized through sol–gel self-assembly in the presence of a nonionic poly(ethylene oxide)–poly(DL-lactic acid-co-glycolic acid)–poly(ethylene oxide) (PEO–PLGA–PEO, EO<sub>16</sub>(L<sub>29</sub>G<sub>7</sub>)EO<sub>16</sub>) triblock copolymer template using boric acid (weak Lewis acid) as a catalyst instead of strong hydrochloric acid. 1,4-Bis(triethoxysilyl)benzene (BTEB) was used as an organosilica precursor, and the reaction and aging temperatures were set at 40 and 100 °C, respectively. The molar concentration of boric acid was varied from 0.5 to 3 M to find the minimum acidity required and to check the effect of this acidic catalyst on the formation of benzene–silica mesostructures. This study shows that the ordered mesostructure of benzene–silica was observed even at 1 M concentration of boric acid ( $[B(OH)_3]/[BTEB] = 12$ ), and highly ordered hexagonal mesostructures were obtained at higher concentrations of this acid. Thermal stability of the benzene–silica materials prepared in the presence of boric acid increased up to 570 °C depending on the amount of this catalyst and exceeded by 20 °C the degradation temperature of the analogous materials obtained with HCl acid. The specific surface areas and pore diameters of the benzene–silicas studied showed values in the range from 833 to 907 m<sup>2</sup> g<sup>−1</sup> and from 6.5 to 8.6 nm, respectively.

**KEYWORDS:** benzene–silica, boric acid, block copolymer templating, periodic mesoporous organosilica, thermal stability



## ■ INTRODUCTION

Since the discovery of mesoporous silica materials prepared by using nonionic poly(ethylene oxide)–poly(propylene oxide)–poly(ethylene oxide) triblock copolymers (Pluronics) as soft templates,<sup>1</sup> numerous mesostructures have been synthesized by employing different types of surfactants and block copolymers.<sup>2</sup> The well-known SBA-type mesoporous materials such as SBA-15 and SBA-16 have been prepared with Pluronic P123 and F127 nonionic block copolymers, and these materials were synthesized under strongly acidic conditions using hydronium ion-generating hydrochloric acid and sulfuric acid.<sup>1</sup> The interactions between hydrophilic poly(ethylene oxide) block of nonionic Pluronic templates and alkoxide-containing silica sources have been identified as hydrogen bond and electrostatic interactions.<sup>3</sup> To obtain highly ordered mesostructures through sol–gel assembly mediated via hydrogen bond interactions, relatively strong acids (pH < 2) are needed, and the required acidity strength depends on the silica/organosilica sources when similar nonionic Pluronic block copolymers are employed.<sup>1,4</sup> For instance, periodic mesoporous organosilica (PMO) materials obtained by using organo-bridged silsesquioxane precursors could be assembled under weaker acidic conditions than purely siliceous mesoporous materials.<sup>2,5</sup> Moreover, the optimal acidity for obtaining highly ordered mesostructures depends on the kind of organic bridging groups.<sup>5</sup> It is known<sup>5</sup> that the formation of an ordered mesostructure by self-assembly of block copolymers and silica species

depends strongly on the properties of the precursors used and the interfacial interactions, which can be quantitatively expressed by the change in the Gibbs free energy.<sup>6</sup> Several reports indicate that PMOs with aromatic bridging groups can be prepared under milder acidic conditions (e.g., using aluminum chloride as an acid catalyst) when more hydrophobic block copolymer templates are employed.<sup>7</sup>

Boron is known to generate weaker acidity than aluminum analogues, and the solid catalyst containing boron species may give interesting results for any specific catalytic reaction. Thus, several reports show that the boron-containing zeolite and mesoporous materials are often used as a source of weak acidity.<sup>8</sup> Boric acid (B(OH)<sub>3</sub>), as a Lewis acid (pK<sub>a</sub> = 9.237), interacts with water molecules to form tetrahydroxyborate anion and hydronium cation (i.e., B(OH)<sub>4</sub><sup>−</sup> + H<sub>3</sub>O<sup>+</sup>), which indicates that boric acid can be used as an acidic catalyst for the formation of mesostructures.<sup>9</sup> On the other side, boron species have been used to prepare monofilament and fiber-glass with silica materials because boron oxides possess excellent hardness, thermal property, and nonlinear optical property.<sup>10</sup> Since the demand for new heteroatom-incorporated mesoporous silica/organosilica materials is increasing, there is a growing interest in boron-containing

Received: January 18, 2011

Revised: March 1, 2011

Published: March 15, 2011

**Table 1.** Physicochemical Properties of 2D Hexagonally Ordered Benzene–Silicas Prepared by Using LGE538 PEO–PLGA–PEO Block Copolymer Template and Boric Acid.<sup>a</sup>

sample	[B(OH) <sub>3</sub> ] (M)	<i>f</i> <sub>BA/BTEB</sub>	pH			<i>S</i> <sub>BET</sub> (m <sup>2</sup> g <sup>−1</sup> )	<i>V</i> <sub>t</sub> (cm <sup>3</sup> g <sup>−1</sup> )	<i>V</i> <sub>c</sub> (cm <sup>3</sup> g <sup>−1</sup> )	<i>V</i> <sub>m</sub> (cm <sup>3</sup> g <sup>−1</sup> )	<i>D</i> <sub>KJS</sub> (nm)	<i>a</i> (nm)	<i>W</i> (nm)
			25 °C	40 °C	100 °C							
LBB-0.5	0.5	6	4.77	4.71	4.52							
LBB-1	1.0	12	4.62	4.56	4.37	855	0.79	0.26	0.52	8.2	10.6	2.4
LBB-1.5	1.5	18	4.53	4.47	4.27	833	0.84	0.22	0.62	8.6 (6.8)	11.3	2.7
LBB-2	2.0	24	4.47	4.41	4.22	851	0.74	0.26	0.46	7.8 (6.5)	10.5	2.7
LBB-2.3	2.3	27	4.44	4.38	4.19	843	0.69	0.26	0.41	6.9	10.2	3.3
LBB-2.5	2.5	30	4.42	4.36	4.18	907	0.94	0.23	0.70	8.4 (7.3)	10.6	2.2
LBB-3	3.0	36	4.38	4.32	4.14	864	0.78	0.25	0.52	7.4	10.4	3.0

<sup>a</sup> Notation: [B(OH)<sub>3</sub>], molar concentration of boric acid in the synthesis gel; *f*<sub>BA/BTEB</sub>, molar ratio of boric acid to 1,4-bis(triethoxysilyl)benzene used in the synthesis gel; pH, pH values of the synthesis gel at respective temperatures of 25 °C, 40 °C, and 100 °C. These values were calculated using *K*<sub>a</sub> obtained via the van't Hoff equation ( $d \ln K_a/dT = \Delta_r H^\circ/RT^2$ ) and ref data under standard conditions (i.e.,  $\Delta_r H^\circ = 13.8$  kJ/mol).<sup>12</sup> Errors are negligible in the small range of 4.1–4.8; *S*<sub>BET</sub>, BET specific surface area determined in the range of relative pressures from 0.04 to 0.2; *V*<sub>t</sub>, single-point pore volume; *V*<sub>c</sub>, volume of complementary pores obtained by integration of PSD up to 4 nm; *V*<sub>m</sub>, volume of mesopores obtained by integration of PSD from 4 to 20 nm; *D*<sub>KJS</sub>, mesopore diameter at the maximum of the PSD curve obtained by the improved KJS method and the value in parentheses obtained from smaller peak of bimodal PSD;<sup>11</sup> *a*, unit cell parameter; *W*, pore wall thickness = *a* − *D*<sub>KJS</sub>; the row for LBB-0.5 has several empty cells because adsorption was not measured for this sample.

materials because boron is one of the interesting elements that has not been fully exploited. Therefore, it would be interesting not only to study the possibility of using a very weak boric acid as an acidic catalyst for the synthesis of ordered mesostructures in the presence of more hydrophobic polymeric templates with higher conformational energy in order to facilitate the formation of ordered mesodomains but also to search for new mesoporous materials with incorporated boron even if it is very difficult to obtain the stable chemical linkage of B–O–Si under acidic conditions.<sup>9</sup>

Here we report the effect of boric acid on the formation of 2D hexagonally ordered benzene–silica mesostructures by employing 1,4-bis(triethoxysilyl)benzene (BTEB) organosilane and a PEO–PLGA–PEO triblock copolymer, which was used to provide additional  $\pi$ – $\pi$  and hydrophobic interactions to control the self-assembly kinetics and to balance the energy of interactions weakened by using boric acid catalyst. The amount of boric acid was varied in the range of 0.5–3 M to find the minimum acidity required for obtaining the ordered mesostructures by self-assembly of PEO–PLGA–PEO and BTEB. In addition, this study shows that there are still possibilities to find new ways for controlling supramolecular interactions between the polymer template and the organosilanes used.

## EXPERIMENTAL SECTION

**Materials.** A commercial Pluronic P123 (EO<sub>20</sub>PO<sub>70</sub>EO<sub>20</sub>) and a poly(ethylene oxide)–poly(DL-lactic acid-co-glycolic acid)–poly(ethylene oxide) triblock copolymer EO<sub>16</sub>(L<sub>29</sub>G<sub>7</sub>)EO<sub>16</sub>, LGE538 were used as polymer templates.<sup>4e,5c</sup> The average molecular weight of the LGE538 block copolymer was 5310, and the polydispersity index was 1.28 by using a GPC-RI (Waters HPLC) system. The molecular weight estimated by <sup>1</sup>H NMR was 4220 Da, and the volume fraction of the PEO blocks ( $\Phi_{\text{PEO}}$ ) was calculated as 0.38 by the group contribution method on the basis of the molar composition obtained by the NMR analysis.<sup>4e,5c</sup>

1,4-Bis(triethoxysilyl)benzene (BTEB, Aldrich) was used as an organosilica precursor, and boric acid (B(OH)<sub>3</sub>, Aldrich) was used as a substitute of acid catalyst instead of a typical proton-containing acid like hydrochloric acid or sulfuric acid.

## Preparation of Periodic Mesoporous Benzene–Silica Using Boric Acid as a Catalyst.

In a typical synthesis of benzene–silica (e.g., LBB-1 in Table 1), 0.5 g of LGE538 triblock copolymer was dissolved in a mixture of 22.0 g of distilled water and 0.5 g of ethanol, and after stirring the polymer solution for 2 h, 0.75 g of BTEB and 1.39 g of B(OH)<sub>3</sub> were added sequentially without any time lag. The mixture was stirred for 20 h at 40 °C followed by aging for 24 h at 100 °C. For this sample the precipitate was formed in the hydrothermal aging step at 100 °C; similar behavior was observed for the LBB-0.5 sample listed in Table 1. For the other LBB samples prepared by using higher amounts of B(OH)<sub>3</sub> than 1 M, the precipitates were formed during the initial synthesis step at 40 °C, that is, before the hydrothermal aging step at 100 °C. To remove the block copolymer template and nonreacted species, 60 g of acetone was used as a washing solvent under magnetic stirring for 24 h at 56 °C. An analogous route was used for the synthesis of other samples listed in Table 1, except for the molar concentrations of boric acid, which were varied as shown in Table 1.

In a typical synthesis of benzene–silica (e.g., PBB-1 in Supporting Information Figure S1) in the presence of a Pluronic P123 polymer template, 0.66 g of P123, 24.0 g of distilled water, 1.48 g of B(OH)<sub>3</sub>, and 0.67 g of BTEB were used. The other synthesis steps were analogous as in the case of the LBB PMOs.

**Measurements and Calculations.** The small-angle X-ray scattering (SAXS) experiments were performed on a Bruker Nanostar U instrument using a Cu K $\alpha$  radiation (with  $\lambda = 1.5418$  Å) source, which was a rotating anode. Each sample was placed in a hole of an aluminum sample holder and secured on both sides using a Kapton tape. The wide-angle X-ray diffraction (WAXD) measurements were performed using a PANalytical X'Pert Pro Multipurpose Diffractometer with Cu K $\alpha$  radiation at 40 kV and 40 mA. The samples were ground manually and put on the microscope glass holder at room temperature. The spectra were collected versus  $2\theta$  from 5° to 65°.

The TEM images were obtained with an FEI Tecnai G2 Twin microscope operated at an accelerating voltage of 120 kV. The samples were sonicated for 30 min in an adequate quantity of ethanol, and the solution was dropped onto a porous carbon film on a copper grid and then dried. The SEM images were obtained with a field emission SEM (JEOL JSM-6300F) operated at an accelerating voltage of 25 kV.

Nitrogen adsorption–desorption isotherms were measured at −196 °C on a Micromeritics 2010 analyzer. The samples were degassed at 120 °C under vacuum below 30  $\mu$ m Hg for at least 2 h before

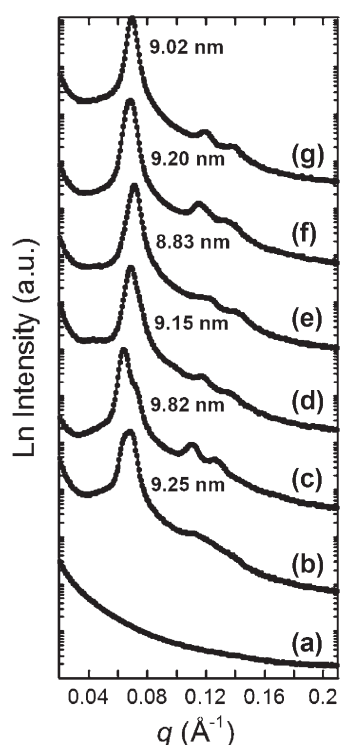


**Figure 1.** SAXS patterns for benzene-silicas prepared using LGE538 triblock copolymer, BTEB, and boric acid. The sequence of the SAXS patterns from (a) to (g) corresponds to the list of samples in Table 1: (a) LBB-0.5, (b) LBB-1, (c) LBB-1.5, (d) LBB-2, (e) LBB-2.3, (f) LBB-2.5, and (g) LBB-3, respectively.

measurement. The BET (Brunauer–Emmet–Teller) specific surface area was calculated from the adsorption data in the relative pressure range from 0.04 to 0.2. The total pore volume was evaluated from the amount adsorbed at a relative pressure of 0.99. The volume of complementary (fine) pores was estimated by integration of pore size distribution (PSD) up to 4 nm, and the mesopore volume was obtained by taking PSD from 4 to 20 nm. The PSD curves were calculated from the adsorption branches of the isotherms by using the improved KJS (Kruk–Jaroniec–Sayari) method.<sup>11</sup> The pore wall thickness was estimated from the pore size obtained at the maximum of PSD and the unit cell parameter ( $a$ ) obtained by SAXS.

Thermogravimetric (TG) measurements were performed using a high-resolution mode of the TA Instrument TGA 2950 analyzer. The TG profiles were recorded up to 800 °C in flowing air with a heating rate of 10 °C min<sup>-1</sup>.

Fourier transform infrared (FT-IR) measurements were performed using a Varian 640-IR spectrophotometer. Spectra were recorded at 32 scans with a resolution of 4 cm<sup>-1</sup> using Varian Resolution Pro software.

## RESULTS AND DISCUSSION

Several benzene-silica powder samples were obtained in the presence of LGE538 PEO-PLGA-PEO triblock copolymer template (EO<sub>16</sub>(L<sub>29</sub>G<sub>7</sub>)EO<sub>16</sub>) by varying the molar concentration of boric acid catalyst. The molar concentration of boric acid was varied from 0.5 to 3 M, which correspond to 6–36 molar ratio of boric acid to BTEB organosilica precursor as shown in Table 1. Precipitates of LBB-0.5 and LBB-1 samples were formed during the hydrothermal aging step at 100 °C for 24 h, while the other samples precipitated before the aging step. The 2D SAXS

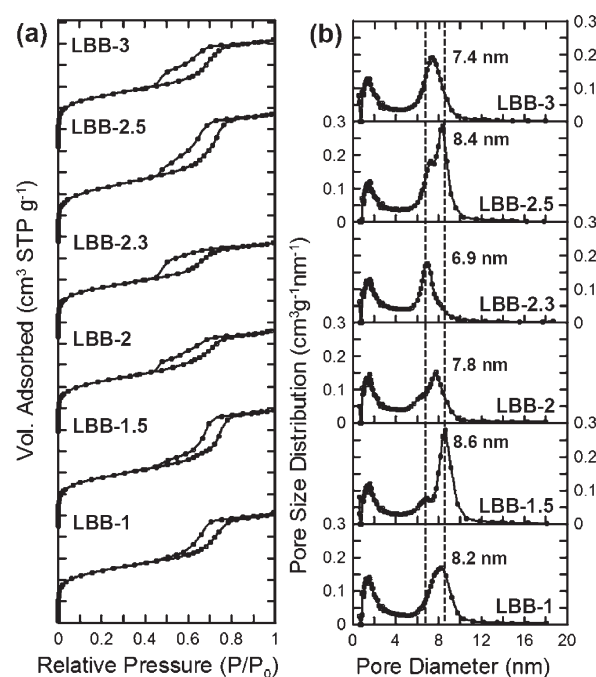


**Figure 2.** Nitrogen adsorption-desorption isotherms and the corresponding pore size distributions for benzene-silicas prepared using LGE538 triblock copolymer, BTEB, and boric acid. The sample names at respective adsorption isotherms and PSDs are listed inside.

patterns for benzene-silicas are shown in Figure 1. As can be seen from this figure, all template-free benzene-silica samples except for LBB-0.5 (curve a in Figure 1) show 2D hexagonal ( $p6mm$ ) ordering. The LBB-1 sample (curve b in Figure 1) is not a highly ordered mesostructure (i.e., the third (200) reflection is not well pronounced). However, all the other samples show at least three well-resolved peaks indexed as the (100), (110), and (200) reflections, which means that the benzene-silica samples obtained using higher amounts of boric acid (>1 M) are highly ordered mesoporous structures. Exceptionally, the SAXS pattern (c) in Figure 1 suggests the presence of a trace amount of another phase in the LBB-1.5 sample. The  $d$ -spacing values obtained from the most intense Bragg peaks vary slightly from 8.83 to 9.82 nm, which does not correlate with the concentration of boric acid. On the other hand, the benzene-silica samples templated by Pluronic P123 block copolymer in the presence of large quantities of boric acid, precipitated during the hydrothermal aging step, did not show the ordered mesostructure (see Supporting Information Figure S1). The white solid product and the confirmation of 2D hexagonal mesostructure of the LBB samples clearly show the effect of highly hydrophobic block copolymer, which even under very weak acidic conditions gave ordered benzene-silica mesostructures.

Nitrogen adsorption-desorption isotherms for benzene-silicas prepared in the presence of a LGE538 block copolymer and boric acid are shown in Figure 2. All the isotherms of the benzene-silica samples are type IV showing distinct hysteresis in a broad range of  $P/P_0$  from 0.40 to 0.80. The BET surface areas for these benzene-silicas are in the range from 833 to 907 m<sup>2</sup> g<sup>-1</sup>, and the total pore volumes ( $V_t$ ) vary from 0.69 to 0.94 cm<sup>3</sup> g<sup>-1</sup> as listed in Table 1. The pore size distributions were calculated by the improved KJS method, which for several



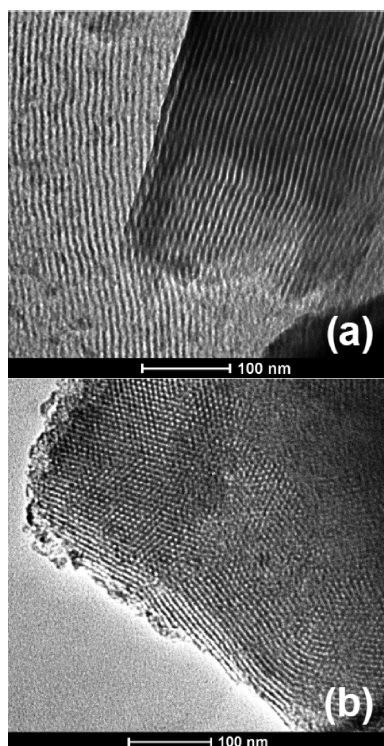


**Figure 3.** Representative TEM images of benzene-silicas prepared using LGE538 triblock copolymer, BTEB, and boric acid without HCl addition: (a) LBB-1 and (b) LBB-3.

benzene-silica samples are bimodal as shown in Figure 2. The pore diameters estimated from the PSD curves are in the range between 6.5 and 8.6 nm. The mesopore diameters obtained at the maximum of the PSD curve are listed in Table 1. Accordingly, the wall thicknesses vary from 2.2 to 3.3 nm. The complementary pore volume ( $V_c$ ) for the pore diameters below 4 nm is nearly the same for the samples studied ( $0.22\text{--}0.26\text{ cm}^3\text{ g}^{-1}$ ). The mesopore volumes corresponding to the range of  $4\text{ nm} \leq D_{KJS} \leq 20\text{ nm}$  vary from  $0.41$  to  $0.70\text{ cm}^3\text{ g}^{-1}$ . The SAXS and nitrogen adsorption analysis indicates that the ordered  $p6mm$  mesoporous benzene-silica can be prepared using at least 1 M of boric acid in the presence of PEO-PLGA-PEO block copolymer template. Also, it is noteworthy that the amount of boric acid is not so important to improve the quality of mesostructure and the porosity, which implies that a very low acidity ( $\text{pH} \approx 4.5$ ) is sufficient for the structure formation. It seems that acidity varies slightly (i.e., 4.1–4.5, Table 1) when a very weak boric acid is used in the range of 1–3 M; higher amount of this acid is not advisable because it is not fully dissolved under the conditions studied.

The  $p6mm$  hexagonal mesostructures of benzene-silicas prepared in the presence of boric acid were also confirmed by the TEM images as shown in Figure 3. Figure 3a shows the cylindrical mesostructured pattern for the LBB-1 sample, and Figure 3b shows a hexagonal pattern for the LBB-3 sample. The SEM images reveal that the overall macroscopic morphology of benzene-silicas is not uniform, as shown in Supporting Information Figure S2, which is mainly attributed to very weak acidic conditions.

The WAXD patterns for benzene-silicas (Figure 4) provide information about structural ordering of the pore walls framework.

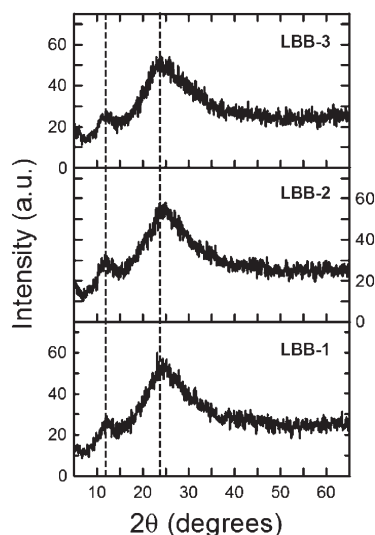


**Figure 4.** Wide angle X-ray diffraction patterns of the LBB-1, LBB-2, and LBB-3 benzene-silica samples prepared using LGE538 triblock copolymer, BTEB, and boric acid.

The two diffraction peaks correspond to the  $d$ -spacings of 0.74 nm ( $2\theta = 12^\circ$ ) and 0.37 nm ( $2\theta = 24.0^\circ$ ), which are assigned to a periodic arrangement of benzene bridging groups linked with silica within the pore walls;<sup>13</sup> however, weak and broad peaks suggest the lack of the crystalline phase, which is typical for the benzene-silica prepared in the presence of nonionic block copolymer templates under acidic conditions.

The TG and DTG profiles show that the benzene-silica materials are thermally stable slightly over  $550^\circ\text{C}$  as shown in Figure 5a. Moreover, a closer analysis reveals that the degradation temperatures vary with the amount of boric acid. Figure 5b shows that the LBB samples prepared with boric acid are more stable than the ordered benzene-silica (LB) sample obtained in a typical 0.1 M HCl solution.<sup>5c</sup> For example, the thermal degradation of the LB sample starts at  $550^\circ\text{C}$  and ends at  $562^\circ\text{C}$ . The maximum degradation rate (i.e., the maximum of the DTG peak) is observed at  $555^\circ\text{C}$ . For the LBB samples, the LBB-3 sample degrades from  $572$  to  $585^\circ\text{C}$ . The maximum rate is observed at  $577^\circ\text{C}$ , which is higher by  $20^\circ$  compared to that of the LB sample. Moreover, the increase in the degradation temperature is dependent on the amount of the boric acid used. The maximum degradation temperatures for the LBB-1 and LBB-2 samples are observed at  $567$  and  $572^\circ\text{C}$ , respectively. A slight enhancement in the thermal stability of the LBB samples is observed with increasing concentration of the boric acid added. The theoretical benzene/silica molar ratio is 1:2 when only 1,4-bis(triethoxysilyl)benzene (BTEB) is used as an organosilica precursor. In this case, the TG weight loss of the benzene-silica material from  $100$  to  $800^\circ\text{C}$  should be around 33.3 wt % in air flow when the ideal  $T^3$  linkage ( $-\text{O}_3\text{Si}-\text{C}_6\text{H}_4-\text{SiO}_3-$ ) is achieved and all the phenylene groups are replaced by oxygen atoms like  $-\text{O}_3\text{Si}-\text{O}-\text{SiO}_3-$  during this thermal treatment. The final TG weight losses in Figure 5 were found as 38.2, 34.5, 34.1, and 33.8 wt % for LB, LBB-1, LBB-2, and LBB-3 samples, respectively, which indicates the benzene/silica ratios in the PMOs studied are close to the theoretical value of 1:2. Also, it is noteworthy that the LBB samples obtained in the presence of boric acid show better thermal stability than typical mesoporous benzene-silicas. From the TG data, it is apparent that the

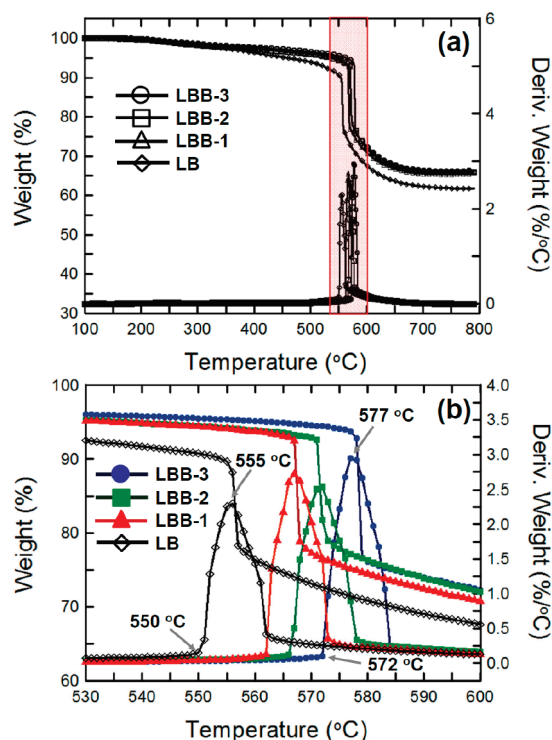


**Figure 5.** (a) Thermogravimetric (TG) and the corresponding differential TG profiles for the representative LBB benzene–silica samples studied in flowing air. The LB sample was prepared using 0.1 M HCl acidic solution in the presence of LGES38 template (reference sample). (b) Enlarged TG and DTG profiles in the selected temperature region.

increase of the thermal stability is caused by boric acid. It is possible to suggest the following explanation: (i) the effect of chemically bonded boric acid with benzene–silica inside the pore wall, and (ii) the role of boric acid as a catalyst to enhance the strength of linkages between benzene–silica precursors during the sol–gel assembly.

To verify the role of boric acid and whether it was a source for boron incorporation into the benzene–silica framework or only an acid catalyst, Fourier transform infrared (FT-IR) as well as EDS (energy dispersive spectroscopy) spectra were recorded. The SEM-EDS analysis has not shown any trace of boron species (data not shown). The characteristic bands of B–O–Si may appear at 920–930 and 1380–1400  $\text{cm}^{-1}$  for tetra- and tricoordinated boron species, respectively.<sup>8</sup> However, the IR peaks in these ranges are attributed to Si–O and –Si–C<sub>6</sub>H<sub>4</sub>–Si– (benzene–silica) based on the peaks of the LB reference sample as shown in Figure 6. Considering the spectrum of the LB sample, the peaks at 808, 913, 1040, and 1150  $\text{cm}^{-1}$  can be assigned to symmetric Si–O–Si and Si–OH and asymmetric Si–O bonds, respectively, as depicted in Figure 6. The peaks at 873 and 1375  $\text{cm}^{-1}$  can be assigned to  $\nu_{10}$  and  $\nu_{19}$  of benzene-bridging groups in benzene–silica.<sup>14</sup> Figure 6 confirms that the boron species are not detectable in the recorded FT-IR spectra. Thus, the primary role of boric acid is to catalyze the self-assembly of the BTEB organosilica precursor and nonionic PEO–PLGA–PEO block copolymer template. It is known that the thermally stable borosilicate glasses (e.g., DURAN and PYREX) contain at least 5% of boron to show higher thermal stability than general silica glasses. Therefore, it seems that the enhanced thermal stability is due to the additional role of boric

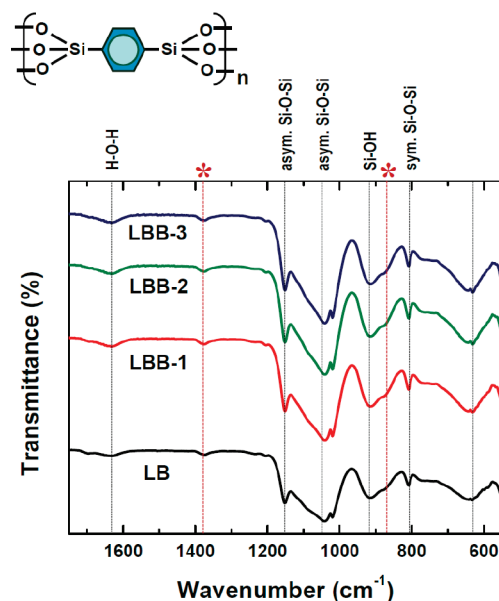


**Figure 6.** FT-IR spectra for the representative benzene–silica samples studied. The LB sample was prepared using 0.1 M HCl acidic solution in the presence of LGES38 template as a reference sample. Asterisks refer to phenylene group in benzene–silica linkage.<sup>14</sup> The top part of this figure shows the chemical structure of benzene–silica.

acid, which suggests that the stability and strength of C–Si–O–Si–C chemical linkages can be somewhat dependent on the reaction environment.<sup>15</sup>

## CONCLUSIONS

The minimum amount of boric acid required for the synthesis of hexagonally ordered mesoporous benzene–silica materials was quite large,  $[\text{B}(\text{OH})_3]/[\text{BTEB}] \approx 12$  (1 M boric acid solution) at 100 °C in the presence of a PEO–PLGA–PEO (EO<sub>16</sub>(L<sub>29</sub>G<sub>7</sub>)EO<sub>16</sub>) block copolymer template. The pH and the molar concentration of hydronium ion at the minimum concentration were calculated as 4.5 and  $3.2 \times 10^{-5}$  M, respectively. Up to 3 M boric acid solution, highly ordered *p6mm* mesoporous benzene–silica samples were obtained; however, the Pluronic P123 block copolymer template did not give an ordered mesostructure. Moreover, the benzene–silica samples prepared in the presence of boric acid showed high thermal stability up to 570 °C, which is higher by 20 °C than that of the sample obtained by using a hydrochloric acid. Also, the thermal stability increased with increasing amount of the boric acid used. This study shows clearly that the highly ordered benzene–silicas can be prepared using different nonionic poly(ethylene oxide)-containing block copolymer templates under very weak acidic conditions. Furthermore, this study implies that different acidic catalysts can be employed in the synthesis of PMOs, and their proper selection can be used to control the self-assembly process and to modify the structural properties of the resulting PMOs.

## ASSOCIATED CONTENT

**S Supporting Information.** Two figures showing the SAXS patterns of the reference benzene–silica samples and SEM images of the LBB benzene–silicas (PDF). This material is available free of charge via the Internet at <http://pubs.acs.org>.

## ■ AUTHOR INFORMATION

## Corresponding Author

\*Phone: 1-330-672 3790. E-mail: jaroniec@kent.edu.

## ■ ACKNOWLEDGMENT

M.J. acknowledges support by the National Science Foundation under Grant CHE-0848352. The authors thank Prof. M. Kruk for discussion, and Prof. Chanjoong Kim for assistance in SEM analysis, Prof. D.-K. Lee and Dr. Woon Kyeom Kim for assistance in FT-IR measurements.

## ■ REFERENCES

- (1) (a) Zhao, D.; Feng, J.; Huo, Q.; Melosh, N.; Fredrickson, G. H.; Chmelka, B. F.; Stucky, G. D. *Science* **1998**, 279, 548–552. (b) Zhao, D.; Huo, Q.; Feng, J.; Chmelka, B. F.; Stucky, G. D. *J. Am. Chem. Soc.* **1998**, 120, 6024–6036.
- (2) (a) Yu, C.; Yu, Y.; Zhao, D. *Chem. Commun.* **2000**, 575–576. (b) Yu, K.; Hurd, A. J.; Eisenberg, A.; Brinker, C. J. *Langmuir* **2001**, 17, 7961–7965. (c) Simon, P. F. W.; Ulrich, R.; Spiess, H. W.; Wiesner, U. *Chem. Mater.* **2001**, 13, 3464–3486. (d) Zhu, H.; Jones, D. J.; Zajac, J.; Rozière, J.; Dutartre, R. *Chem. Commun.* **2001**, 2568–2569. (e) Muth, O.; Schellbach, C.; Fröba, M. *Chem. Commun.* **2001**, 2032–2033. (f) Cho, E.-B.; Kwon, K.-W.; Char, K. *Chem. Mater.* **2001**, 13, 3837–3839. (g) Burleigh, M. C.; Markowitz, M. A.; Wong, E. M.; Lin, J.-S.; Gaber, B. P. *Chem. Mater.* **2001**, 13, 4411–4412. (h) Yang, S.; Mirau, P. A.; Pai, C.-S.; Nalamasu, O.; Reichmanis, E.; Lin, E. K.; Lee, H.-J.; Gidley, D. W.; Sun, J. *Chem. Mater.* **2001**, 13, 2762–2764. (i) Chang, L.-Q.; Wang, J. H.; Shin, Y.; Jeong, B.; Birnbaum, J. C.; Exarhos, G. J. *Adv. Mater.* **2002**, 14, 378–382. (j) Matos, J. R.; Mercuri, L. P.; Kruk, M.; Jaroniec, M. *Langmuir* **2002**, 18, 884–890. (k) Matos, J. R.; Kruk, M.; Mercuri, L. P.; Jaroniec, M.; Asefa, T.; Coombs, N.; Ozin, G. A.; Kamiyama, T.; Terasaki, O. *Chem. Mater.* **2002**, 14, 1903–1905.
- (3) (a) Soler-Illia, G. J.; de, A. A.; Sanchez, C.; Lebeau, B.; Patarin, J. *Chem. Rev.* **2002**, 102, 4093–4138. (b) Wan, Y.; Zhao, D. *Chem. Rev.* **2002**, 107, 2821–2860.
- (4) (a) Liu, X.; Tian, B.; Yu, C.; Gao, F.; Xie, S.; Tu, B.; Che, R.; Peng, I.; Zhao, D. *Angew. Chem., Int. Ed.* **2002**, 41, 3876–3878. (b) Fan, J.; Yu, C.; Gao, T.; Lei, J.; Tian, B.; Wang, I.; Luo, Q.; Tu, B.; Zhou, W.; Zhao, D. *Angew. Chem., Int. Ed.* **2003**, 42, 3146–3150. (c) Kleitz, F.; Liu, D.; Anilkumar, G.; Park, I. S.; Solovyov, L.; Shmakov, A.; Ryoo, R. *J. Phys. Chem. B* **2003**, 107, 14296–14300. (d) Kleitz, F.; Choi, S. H.; Ryoo, R. *Chem. Commun.* **2003**, 2136–2137. (e) Cho, E.-B.; Char, K. *Chem. Mater.* **2004**, 16, 270–275.
- (5) (a) Goto, Y.; Inagaki, S. *Chem. Commun.* **2002**, 2410–2411. (b) Morell, J.; Woltner, G.; Fröba, M. *Chem. Mater.* **2005**, 17, 804–808. (c) Cho, E.-B.; Kim, D.; Jaroniec, M. *Chem. Mater.* **2008**, 20, 2468–2475. (d) Qiao, S. Z.; Yu, C. Z.; Xing, W.; Hu, Q. H.; Djojoputro, H.; Lu, G. Q. *Chem. Mater.* **2005**, 17, 6172–6176. (e) Zhou, X.; Qiao, S.; Hao, N.; Wang, X.; Yu, C.; Wang, L.; Zhao, D.; Lu, G. Q. *Chem. Mater.* **2007**, 19, 1870–1876.
- (6) (a) Monnier, A.; Schüth, F.; Huo, Q.; Kumar, D.; Margolese, D.; Maxwell, R. S.; Stucky, G. D.; Krishnamurty, M.; Petroff, P.; Firouzi, A.; Janicek, M.; Chmelka, B. F. *Science* **1993**, 261, 1299–1303. (b) Huo, Q.; Margolese, D. I.; Ciesla, U.; Demuth, D. G.; Feng, P.; Gier, T. E.; Sieger, P.; Firouzi, A.; Chmelka, B. F.; Schüth, F.; Stucky, G. D. *Chem. Mater.* **1994**, 6, 1176–1191.
- (7) (a) Zhang, L.; Yang, Q.; Zhang, W.-H.; Li, Y.; Yang, J.; Jiang, D.; Zhu, G.; Li, C. J. *Mater. Chem.* **2005**, 15, 2562–2568. (b) Cho, E.-B.; Kim, D.; Górka, J.; Jaroniec, M. *J. Phys. Chem. C* **2009**, 113, 5111–5119.
- (8) (a) Fild, C.; Shantz, D. F.; Lobo, R. F.; Koller, H. *Phys. Chem. Chem. Phys.* **2000**, 2, 3091–3098. (b) Trong, O. N.; Joshi, P. N.; Kaliaguine, S. *J. Phys. Chem.* **1996**, 100, 6743–6748. (c) Yuan, Z. Y.; Luo, Q.; Liu, J. Q.; Chen, T. H.; Wang, J. Z.; Li, H. X. *Microporous Mesoporous Mater.* **2001**, 42, 289–297. (d) Hwang, S.-J.; Chen, C.-Y.; Zones, S. I. *J. Phys. Chem. B* **2004**, 108, 18535–18546. (e) Koller, H.; Fild, C.; Lobo, R. F. *Microporous Mesoporous Mater.* **2005**, 79, 215–224. (f) Wang, D.-W.; Li, F.; Chen, Z.-G.; Lu, G. Q.; Cheng, H.-M. *Chem. Mater.* **2008**, 20, 7195–7200. (g) Hunt, J. R.; Doonan, C. J.; LeVangie, J. D.; Côté, A. P.; Yaghi, O. M. *J. Am. Chem. Soc.* **2008**, 130, 11872–11873. (h) Xu, Y.; Wu, Z.; Zhang, L.; Lu, H.; Yang, P.; Webley, P. A.; Zhao, D. *Anal. Chem.* **2009**, 81, 503–508.
- (9) (a) Goldberg, S. J. *Colloid Interface Sci.* **2005**, 285, 509–517. (b) Ding, S.; Liu, N.; Li, X.; Peng, L.; Guo, X.; Ding, W. *Langmuir* **2010**, 26, 4572–4575.
- (10) (a) El-Kaderi, H. M.; Hunt, J. R.; Mendoza-Cortes, J. L.; Côté, A. P.; Taylor, R. E.; O’Keeffe, M.; Yaghi, O. M. *Science* **2007**, 316, 268–272. (b) Han, Z.; Li, G.; Tian, J.; Gu, M. *Mater. Lett.* **2012**, 57, 899–903. (c) Buc, D.; Bello, I.; Caplovicova, M.; Mikula, M.; Kovac, J.; Hotovy, I.; Chong, Y. M.; Siu, G. G. *Thin Solid Films* **2007**, 515, 8723–8727.
- (11) Jaroniec, M.; Solovyov, L. A. *Langmuir* **2006**, 22, 6757–6760.
- (12) Goldberg, R. M.; Kishore, N.; Lennen, R. M. *J. Phys. Chem. Ref. Data* **2002**, 31, 231–370.
- (13) Inagaki, S.; Guan, S.; Ohsuna, T.; Terasaki, O. *Nature* **2002**, 416, 304–307.
- (14) Onida, B.; Borello, L.; Busco, C.; Ugliengo, P.; Goto, Y.; Inagaki, S.; Garrone, E. *J. Phys. Chem. B* **2005**, 109, 11961–11966.
- (15) Leontidis, E. *Curr. Opin. Colloid Interface Sci.* **2002**, 7, 81–91.